Research article

Journal of RAMAN SPECTROSCOPY

Received: 14 October 2016 Revised: 13 November 2016 Accepted: 18 November 2016 Published online in Wiley Online Library: 8 February 2017

(wileyonlinelibrary.com) DOI 10.1002/jrs.5078

Raman study of $HoFe_3(BO_3)_4$ at simultaneously high pressure and high temperature: *p–T* phase diagram

A. S. Krylov ,[a]* I. A. Gudim,[a] I. Nemtsev ,[a] S. N. Krylova,[a] A. V. Shabanov[a] and A. A. Krylov[b]

Raman spectra of a $HoFe_3(BO_3)_4$ crystal chip has been investigated at simultaneously high temperature and high pressure (up to 7.1 GPa and 560 K). On the basis of Raman analysis, the assignment to one of the two possible crystal phases has been made. The experimental *p–T* phase diagram of $HoFe_3(BO_3)_4$ was established. An increase in the pressure leads to an increase in the temperature of transition. The phase boundary equation was obtained. Neither triple points nor a phase with new symmetry was revealed in the phase diagram. A critical point with the temperature *T* = 560 K and the pressure *p* = 2.53 GPa was found. The nanocrystals with different shapes began to grow on crystal surface after reaching that point. The composition of new nanocrystals is identical to the composition of initial crystal. Copyright © 2017 John Wiley & Sons, Ltd.

Keywords: phase transitions; high hydrostatic pressure; ferroborates; *p–T* phase diagram; nanocrystal

Introduction

In recent years, the crystals of rare-earth ferroborates $ReFe_3(BO_3)_4$ (*Re* – is the rare-earth atom) which belongs to huntite family have attracted much attention.[1–4] The combination of high physical characteristics and chemical stability, the borate with huntite structure have long been used as elements of optical and optoelectronic devices, specifically to add and multiply the laser radiation frequencies[5] application for self-frequency doubling and self-frequency summing lasers[6,7]; rare-earth huntite crystals are efficient media for mini-lasers.[8] Ferroborates were reported to possess multiferroic features, demonstrating the coexistence of magnetic and ferroelectric order parameters.[9] Multiferroic materials showing the coexistence of at least two ferroic orders ((anti)ferroelectric, (anti)ferromagnetic, and (anti)ferroelasticity) are expected to find potential applications in many devices. Among aforementioned properties, the coexistence of ferroelectricity and ferromagnetism is highly desired. Besides their coexistence, utmost importance is a strong coupling between the two ferroic orders. In multiferroic materials, the coupling interaction between the different order parameters can produce additional functionalities. The application of multiferroics will make possible to significantly enlarge the functional possibilities of spintronics devices. In addition, $HoFe_3(BO_3)_4$ are observed to have rather unusual structural phase transition between nonpolar phases of trigonal crystal system (from high-temperature *R*32 ($Z = 1$) into low-temperature $P3_121$ ($Z = 3$), and an addition into the structure of two magnetic ions of different types (3*d* и 4*f*) gives rise to magnetic order at low temperatures.[10] Coexistence of structural and magnetic order parameters can open new opportunities to control their physical characteristics.

The structure in the *R*32 phase of these crystals is too identical as is presented in the works.[11–13] It is formed by two helicoidal chains of FeO_6 octahedra with common edges connected by two types of BO_3 plane triangles with rare-earth ions in the cavities between them. These chains are the same in the *R*32 phase while in the $P3_121$ phase, FeO_6 octahedra are distorted slightly forming two different types of the chains.[14]

The symmetry of the phases on the phase diagram after temperature or pressure phase transition depends on location tricritical point and could be either the same or different.[15–17] Also, it is possible that pressure phase transition exists but temperature phase transition does not occur (negative temperature of virtual phase transition).[18] The study of the phase diagram of the temperature–pressure is very important for materials with practical applications. *In situ* measurements at high *p–T* parameters, are very rare in research works and give unique and important information about the actual state of materials at extreme conditions. The quantity of works devoted to the study of phase diagrams at high temperatures and high pressure increases from year to year, reflecting the importance of these investigations. They are held in a variety of materials: inorganic,[19–21], organic,[22,23] and gas hydrates.[24,25]

The ferroborates with various rear-earth elements traditionally were studied by Raman spectroscopy.[14,26] The temperature phase transition in $HoFe_3(BO_3)_4$ earlier was investigated by high-resolution spectroscopy,[27] IR spectroscopy,[13] Raman spectroscopy,[12] and ab-initio calculations.[28] However, a structural phase transition in holmium ferroborate has never been studied under high hydrostatic pressure. The aim of our work is to

* *Correspondence to: A. S. Krylov , Kirensky Institute of Physics, Federal Research Center, KSC SB RAS, Krasnoyarsk 660036, Russia. E-mail: shusy@iph.krasn.ru*

a *Kirensky Institute of Physics, Federal Research Center, KSC SB RAS, Krasnoyarsk 660036, Russia*

b *Department of Physical and Quantum Electronics, Moscow Institute of Physics and Technology, Dolgoprudny 141700, Russia*

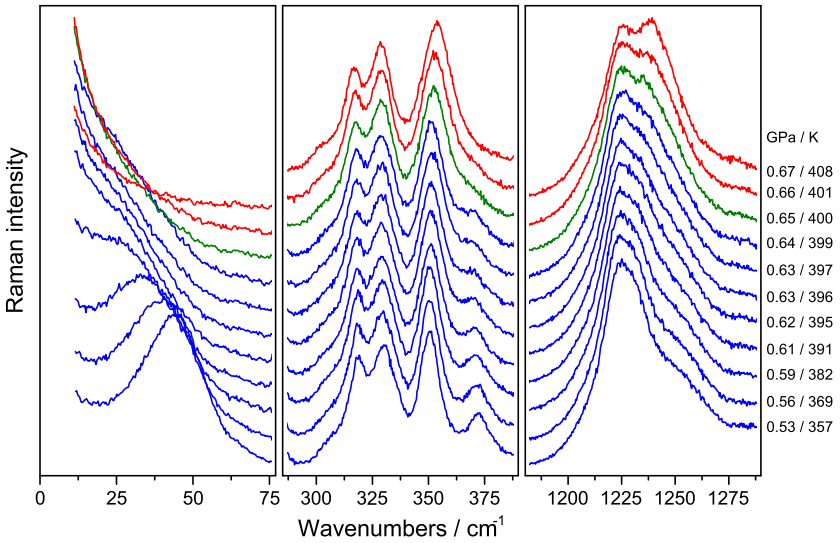

Figure 1. Raman spectra. Color code: red-phase *R*32, blue-phase $P3_121$, olive-phase boundary at 0.65GPa / 400K.

study *p*–*T* phase diagram and possibly find a new structural phase of $HoFe_3(BO_3)_4$ single crystal.

Methods and sample

The spectra in the 180° geometry were recorded on a Horiba Jobin Yvon T64000 spectrometer equipped with a liquid nitrogen cooled charge coupled device detection system in subtractive dispersion mode. Ar^+ ion laser Spectra Physics Stabilite 2017 with $\lambda = 514.5$ nm and power 5 mW on a sample was used as an excitation light source. The high-pressure experiments were carried out using incident laser beam was focused on the sample by a 50× Olympus LMPlanFl objective lens with a numerical aperture N.A. = 0.35. The scattered light was collected by the same objective lens in the backscattering geometry and analyzed through a polarizer and λ-plate. Spectroscopic measurements were performed in the subtractive dispersion mode to investigate the low-wavenumber spectra, which attained a low-wavenumber limit of 8 cm^{-1} in the present setup. The deformation of the low-wavenumber spectral edge by an optical slit, which sometimes smears the true features of low-wavenumber spectra, was carefully eliminated by rigorous optical alignment.

The heated high-temperature diamond anvil cell device (HT-DAC) of membrane Diacell μScope DAC HT(G) type (EasyLab, UK) with diamond IIa anvils, electrical resistive heating, water-cooling casing, and Ar gas blowing was used for Raman study of processes at simultaneously high *p* and *T*. Limit $p--T$ parameters in the work volume of the given HT-DAC are equal to 20 GPa and 800 K. The maximal $p--T$ values in the present experiments with $HoFe_3(BO_3)_4$ were set at 8 GPa and 680 K. A stainless steel gasket with initial thickness 0.25 mm is used in this DAC. Holes with a diameter of about 150–200 μm were drilled in the gaskets pre-indented to a thickness about 86 μm, for measuring at pressures up to 15 GPa. The pressure was monitored by the shift of the $^5D_0 - ^7F_0$ fluorescence band of Sm^{2+} ion in a small $SrB_4O_7:Sm^{2+}$ crystal placed in the vicinity of the sample within the experimental error of about 0.05 GPa.[29–31] The temperature was monitored using a type K thermocouple in contact with the gasket and diamond anvil. A mixture of methanol–ethanol alcohols in 4 : 1 parts has been used as a hydrostatic pressure transmission media.

X-ray semi-quantitative analysis of the sample was carried out on a tabletop scanning electron microscope Hitachi TM-3000 with detector BRUKER XFlash 430 H. The acceleration voltage was 3 kV. The signal came from a 0.2 mm diameter circle.

Single crystal samples were grown by flux melt method from Bi_2Mo_3O12, [12,32,33] this made the substitution of rare-earth ions with bismuth minimal; EDX-spectroscopy analysis showed bismuth in the structure of synthesized samples to be less than 2%. Measurements were carried out with crystals which did not contain visible in microscope defects or inclusions. The chips of $HoFe_3(BO_3)_4$ crystals was used as a sample in high-pressure experiments.

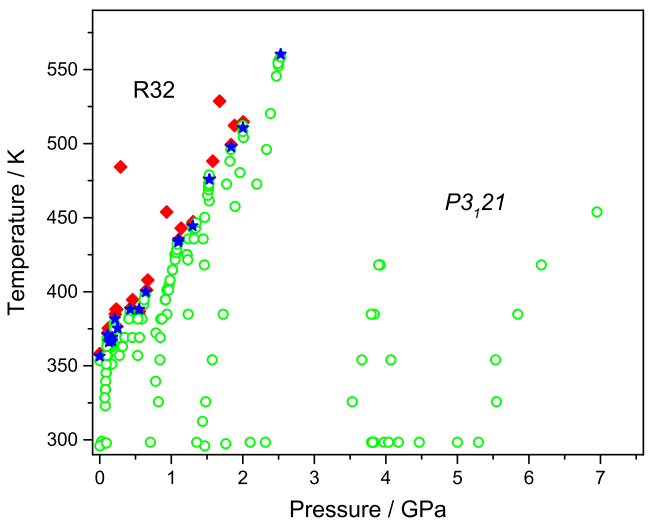

Figure 2. All experimental *p*–*T* points. Color code: red point-phase *R*32, green point-phase $P3_121$, blue-phase boundary.

Results and disscusion

The crystal $HoFe_3(BO_3)_4$ was investigated by Raman spectroscopy in a temperature range from 296 to 560 K and simultaneously under pressure up to 7.1 GPa. We determined the symmetry of crystal phase from Raman spectra during the experiment.

On the basis of previous work,[12] we know changes of the Raman spectrum of the $HoFe_3(BO_3)_4$ crystal at the temperature of phase transition point. Raman spectra transformation with quasi-constant pressure and different temperatures presented in Fig. 1. The phase transition point could be determined by analyzing the sequence of Raman spectra acquired during changing temperature of the resistive heater. The first feature is a structural soft-mode condensation in low-wavenumber region of Raman spectra sequence of $HoFe_3(BO_3)_4$ crystal. The next features are eliminating lines in the middle wavenumber regions and at high wavenumber regions, the corresponding vibration of BO_3 groups. All experiment points according to the assignment to one of phase is presented in Fig. 2. It should be noticed that points belong to the phase *R*32 located lower on pressure scale whereas phase $P3_121$ spread far to the right on pressure scale. During the experiment, we set up some pressure value and successively change the only temperature. The pressure between diamond anvils inside gasket chamber slightly increases because of liquid media volume expansion with temperature increment. Obtained Raman spectra for any pair temperature-pressure of the parameters value could be uniquely assigned to one of three pressure-temperature groups, namely belongs to the phase *R*32, to the phase $P3_121$, or to the phase boundary. While the spectra measuring data, which does not meet any of the groups mentioned previously and belongs to the new phase, were not found.

In our experiment, the temperature was measured by thermocouples in contact with the gasket. The sample temperature could

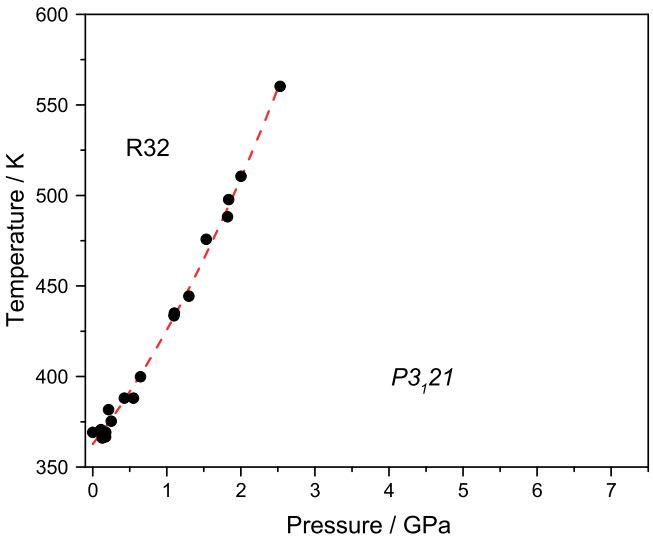

Figure 3. *p–T* phase diagram of $HoFe_3(BO_3)_4$ crystal.

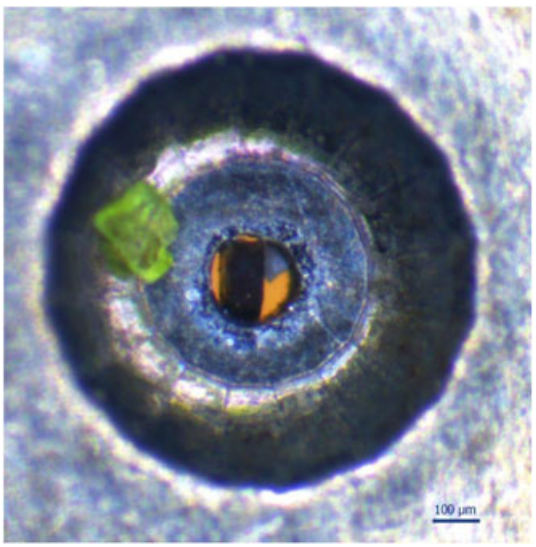

Figure 4. Compare view of initial sample (green) and after experiment (black) in drilled gasket. White crystal-pressure sensor.

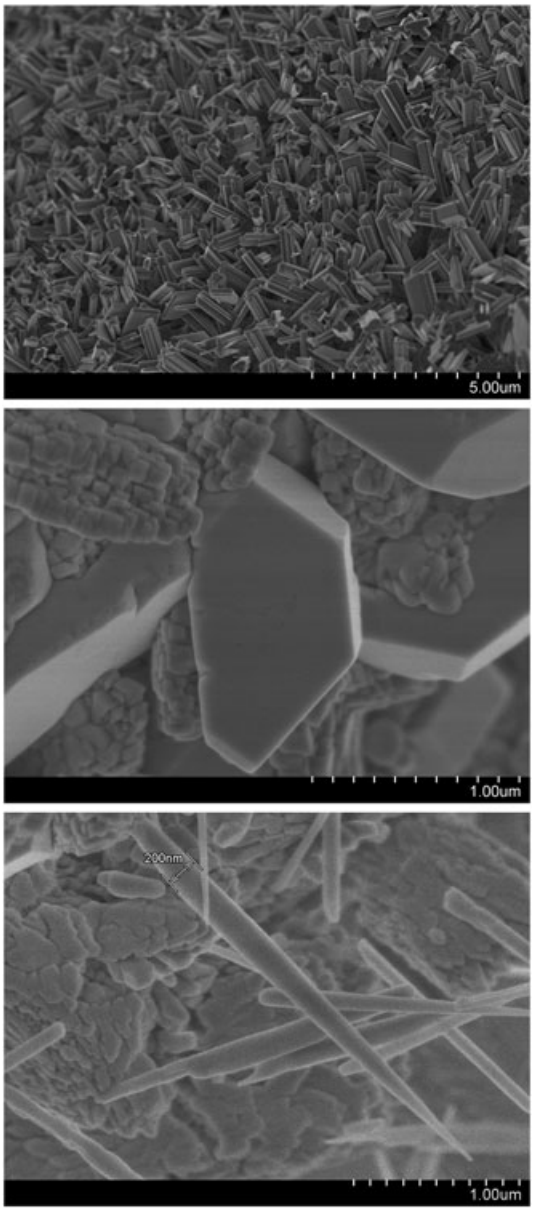

Figure 5. Shapes of newly grown nanocrystals on sample surface after experiment.

Table 1. Compare composition of initial crystal and growth niddle

Initial crystal					Niddle				
El	AN	Series	Norm. C [wt.%]	Atom. C [at.%]	El	AN	Series	Norm. C [wt.%]	Atom. C [at.%]
Fe	26	K-series	36.26	19.68	Fe	26	K-series	31.90	15.66
Ho	67	L-series	28.02	5.15	Ho	67	L-series	27.36	4.55
O	8	K-series	27.47	52.05	O	8	K-series	28.59	48.99
B	5	K-series	8.25	23.12	B	5	K-series	12.15	30.80
		Total:	100.00	100.00			Total:	100.00	100.00

be different from the values measured by the thermocouple. It is generally assumed that the pressure and temperature shifts are independent, such that the measured wavelength shift at a given p–T point is the simple sum of the two contributions.[29,31,34,35] We performed experiments with two pressure sensors for calibrating thermocouple readings. We used small $SrB_4O_7:Sm^{2+}$ crystal as a pressure sensor that does not depend on the temperature and the ruby chip as a sensor reading which depends on the pressure and the temperature. Thus, knowing the shift of the ruby luminescence band, consisting of independent contributions of temperature and pressure and using the reading of the second sensor as a pressure data, we calculated the temperature inside the pressure chamber. Comparing the thermocouple data and the calculated ones, we got a calibration curve.

The experimental p–T phase diagram of the compound under investigation with applying temperature correction is depicted in Fig. 3. An increase in the pressure leads to an increase in the temperatures of transition, and the dependencies $T(p)$ of the boundary between the $R32$ phase and low-temperature $P3_121$ phase could be described adequately with the equation of the type $T(p) = a + bp + cp^2$, where $a = 363.7 \pm 2.1$ K, $b = 52.7 \pm 5.1$ K·GPa^{-1}, and $c = 10.4 \pm 2.2$ K·GPa^{-2}. Therefore, under pressure, the temperature ranges of the $P3_121$ phases increase. No triple points were revealed in the phase diagram.

During research of the phase boundary between two phases, the critical point has been detected. After reaching a critical point with the parameters T= 560 K and the pressure P=2.53 GPa, the spectrum intensity drastically decreased. This transformation was irreversible: Raman spectrum intensity was not restored even when the pressure and temperature were decreased to ambient values. The same behavior could be applied to the crystal's color and transparency. Thus, at this point, the experiment was finished. The sample color and transparency radically changed after reaching the critical point (Fig. 4). The sample surface was studied by the electron microscopy after removing the sample from high-pressure DAC. The new different shapes crystals grown on the surface. The pyramids, needle crystals, natural faceting crystals were found (Fig. 5). To study the surface of the sample more carefully, the investigation was carried out with a scanning electron microscope S-5500 in the Center of the common use of Krasnoyarsk Scientific Center Siberian Branch of Russian Academy of Sciences. We made the two assumptions. The first assumption is the possibility of the phase transition. The second assumption is that the change of the temperature and pressure caused recrystallization on the sample surface. To test these assumptions, etching the surface with argon was performed to obtain a sample surface without newly formed crystals and a re-examination by the Raman spectroscopy. Further investigation by the Raman spectroscopy showed that there was no change in the crystal's original phase. The studies on the microscope Hitachi TM-3000 are presented in the Table 1. We performed EDX-spectroscopy analysis of the needles and initial crystal. Table 1 shows the comparison of the compositions initial samples and a new needle. The main conclusion is that composition of initial crystal and newly grown one are the same.

Conclusions

On the basis of Raman study of $HoFe_3(BO_3)_4$ crystal has been compressed in the alcohol medium at simultaneously high pressure and temperature (up to 7.1 GPa and 560 K). The pressure-temperature phase diagram has been obtained for the first time for ferroborate crystal with rare-earth element atoms based on analyzing Raman spectra. The phase boundary equation was obtained. The critical point with parameters temperature T=570 K and pressure P=2.5 GPa was discovered. Reaching pressure-temperature point with this parameters initiate the growth process of the new nanostructures on the initial crystal surface. It has been found that nanostructures could be different shapes such as rectangular pyramids, needle, and some others. On the basis of EDX-spectroscopy analysis, we conclude that the chemical composition of this new nanocrystals is the same as the composition of the initial crystal.

Acknowledgements

Authors are grateful to Prof. A. N. Vtyurin for his valuable discussion. This work was supported by the Russian Foundation for Basic Research (grant no. 17-02-00694)

References

[1] A. A. Mukhin, G. P. Vorob'ev, V. Y. Ivanov, A. M. Kadomtseva, A. S. Narizhnaya, A. M. Kuz'menko, Y. F. Popov, L. N. Bezmaternikh, I. A. Gudim, *JETP Letters* **2011**, *93*, 275.
[2] C. Ritter, A. Vorotynov, A. Pankrats, G. Petrakovskii, V. Temerov, I. Gudim, R. Szymczak, *J. Phys.: Condens. Matter* **2008**, *20*, 365209.
[3] A. A. Demidov, D. V. Volkov, *Phys. Solid State* **2011**, *53*, 985.
[4] I. A. Gudim, E. V. Eremin, V. L. Temerov, *J. Cryst. Growth.* **2010**, *312*, 2427.
[5] S. A. Klimin, D. Fausti, A. Meetsma, L. N. Bezmaternikh, P. H. M. van Loosdrecht, T. T. M. Palstra, *Acta Crystallogr B Struct Sci* **2005**, *61*, 481.
[6] D. Jaque, *J. Alloys Compd.* **2001**, *204*, 323.
[7] A. Brenier, C. Tu, Z. Zhu, B. Wu, *Appl. Phys. Lett.* **2004**, *84*, 2034.
[8] X. Chen, Z. Luo, D. Jaque, J. J. Romero, J. Garcia Solé, Y. H uang, A. Jiang, C. Tu, *J. Phys.: Condens. Matter* **2001**, *13*, 1171.
[9] A. K. Zvezdin, S. S. Krotov, A. M. Kadomtseva, G. P. Vorob'ev, Y. F. Popov, A. P. Pyatakov, L. N. Bezmaternykh, E. Popova, *JETP Lett* **2005**, *81*, 272.
[10] A. M. Kadomtseva, Y. F. Popov, G. P. Vorob'ev, A. P. Pyatakov, S. S. Krotov, K. I. Kamilov, V. Y. Ivanov, A. A. Mukhin, A. K. Zvezdin, A. M. Kuz'menko, L. N. Bezmaternykh, I. A. Gudim, V. L. Temerov, *Low Temp. Phys.* **2010**, *36*, 511.
[11] A. De Andres, F. Agullo-Rueda, S. Taboada, C. Cascales, J. Campa, C. Ruiz-Valero, I. Rasines, *J. Alloys Compd.* **1997**, *250*, 396 (1997).

[12] A. Krylov, S. N. Sofronova, I. A. Gudim, A. N. Vtyurin, *Solid State Commun.* **2013**, *174*, 26.
[13] Y. V. Gerasimova, S. N. Sofronova, I. A. Gudim, A. S. Oreshonkov, A. N. Vtyurin, A. A. Ivanenko, *Phys. Solid State.* **2016**, *58*, 55–159.
[14] D. Fausti, A. Nugroho, P. Loosdrecht, S. Klimin, M. Popova, L. Bezmaternykh, *Phys. Rev. B* **2006**, *74*, 024403.
[15] A. S. Krylov, S. V. Goryainov, N. M. LaptashI, A. N. Vtyurin, S. V. Melnikova, S. N. Krylova, *Cryst. Growth Des.* **2014**, *14*, 374.
[16] A. S. Krylov, S. V. Goryainov, A. N. Vtyurin, S. N. Krylova, S. N. Sofronova, N. M. Laptash, T. B. Emelina, V. N. Voronov, S. V. Babushkin, *J. Raman Spectrosc.* **2012**, *43*, 577.
[17] A. Krylov, N. Laptash, A. Vtyurin, S. Krylova, *J Mol Struct* **1124**, *2016*, 125.
[18] A. S. Krylov, A. N. Vtyurin, V. D. Fokina, S. V. Goryainov, A. G. Kocharova, *Phys. Solid State* **2006**, *48*, 1064.
[19] D. Errandone, F. J. Manjon, *Prog Mater Sci* **2008**, *53*, 711.
[20] G. Parakhonskiy, N. Dubrovinskaia, E. Bykova, R. Wirth, L. Dubrovinsky, *Sci. Rep.* **2011**, *1*, 96.
[21] Y. M. Ma, Q. Zhou, Z. He, F. F. Li, K. F. Yang, Q. L. Cui, G. T. Zou, *J. Phys.: Condens. Matter* **2007**, *19*, 425221.
[22] S. J. Smith, J. M. Montgomery, Y. K. Vohra, *J. Phys.: Condens. Matter* **2016**, *28*, 035101.
[23] L. Ciabini, F. A. Gorelli, M. Santoro, R. Bini, V. Schettino, M. Mezouar, *Rev. B* **2005**, *72*, 094108.
[24] A. V. Kurnosov, A. G. Ogienko, S. V. Goryainov, E. G. Larionov, A. Y. Manakov, A. Y. Lihacheva, E. Y. Aladko, F. V. Zhurko, V. I. Voronin, I. F. Berger, A. I. Ancharov, *J. Phys. Chem. B* **2006**, *110*, 1788.
[25] A. Y. Manakov, Y. A. Dyadin, A. G. Ogienko, A. V. Kurnosov, E. Y. Aladko, E. G. Larionov, F. V. Zhurko, V. I. Voronin, I. F. Berger, S. V. Goryainov, A. Y. Lihacheva, A. I. Ancharov, *J. Phys. Chem. B* **2009**, *113*, 7257.
[26] E. Moshkina, A. Krylov, S. Sofronova, I. Gudim, V. Temerov, *Cryst. Growth Des.* **2016**, *16*, 6915.
[27] D. A. Erofeev, E. P. Chukalina, L. N. Bezmaternykh, I. A. Gudim, M. N. Popova, *Opt. Spectrosc.* **2016**, *120*, 558.
[28] V. I. Zinenko, M. S. Pavlovskii, A. S. Krylov, I. A. Gudim, E. V. Eremin, *J. Exp. Theor. Phys.* **2013**, *117*, 1032.
[29] F. Datchi, A. Dewaele, P. Loubeyre, R. Letoullec, Y. Le Godec, B. Canny, *High Pressure Res.* **2007**, *27*, 447.
[30] S. V. Rashchenko, A. Y. Likhacheva, T. B. Bekker, *High Pressure Res.* **2013**, *33*, 720.
[31] S. V. Rashchenko, A. V. Kurnosov, L. Dubrovinsky, K. D. Litasov, *J. Appl. Phys.* **2015**, *117*, 145902.
[32] R. P. Chaudhury, F. Yen, B. Lorenz, Y. Y. Sun, L. N. Bezmaternykh, V. L. Temerov, C. W. Chu, *Phys Rev B* **2009**, *80*, 104424.
[33] S. N. Sofronova, Y. V. Gerasimova, A. N. Vtyurin, I. A. Gudim, N. P. Shestakov, A. A. Ivanenko, *Vib. Spectro.* **2014**, *72*, 20.
[34] G. Piermarini, S. Block, J. Barnett, R. A. Forman, *J. Appl. Phys* **1975**, *46*, 2774.
[35] W. L. Vos, J. A. Schouten, *J. Appl. Phys.* **1991**, *69*, 6744.